Asociación Argentina de Mecánica Computacional

Mecánica Computacional Vol XXV, pp. 1767-1779
Alberto Cardona, Norberto Nigro, Victorio Sonzogni, Mario Storti. (Eds.)
Santa Fe, Argentina, Noviembre 2006

COUPLED FREE VIBRATIONS OF TAPERED BOX-BEAMS MADE OF COMPOSITE MATERIALS

Marcelo T. Piovan [a,b], Carlos P. Filipich[a] and Víctor H. Cortínez [a,b]

[a]*Grupo Análisis de Sistemas Mecánicos, Universidad Tecnológica Nacional FRBB, 11 de Abril 461, B8000LMI Bahía Blanca, BA, Argentina,*
mpiovan@frbb.utn.edu.ar, filipich@hotmail.com, vcortine@frbb.utn.edu.ar
[b]*Consejo Nacional de Investigaciones Científicas y Tecnológicas (CONICET)*

Keywords: Thin-walled tapered-beams, Power Series, Composite Materials. Vibration.

Abstract. In this paper, analytical solutions are developed for the free vibration analysis of tapered thin-walled laminated-composite beams with closed cross-sections. The present approach is based in a recently developed model that incorporates in a full form the shear flexibility. The model considers shear flexibility due to bending as well as non-uniform torsional warping. The model is briefly reviewed with the aim to present the equilibrium equations and the related boundary conditions and constitutive equations. The lamination can be selected in order to manifest different types of elastic couplings. The typical laminations for a box-beam, like Circumferentially Uniform Stiffness and Circumferentially Asymmetric Stiffness stacking sequences, are analyzed.
The exact values (i.e. with arbitrary precision) of frequencies are obtained by means of power series schemes. A parametric analysis is performed for different taper ratios, stacking sequences and materials.

1 INTRODUCTION

Composite materials have many advantages with respect to isotropic materials that motivate their use in structural components. The most well known properties of composite materials are high strength and stiffness properties along with a low weight, good corrosion resistance, enhanced fatigue life and low thermal expansion properties among others (Barbero, 1999). Other important feature of composite materials is its very low machining cost in comparison with isotropic material (Jones, 1999). As a result of the increasing employment of composite thin-walled beams, the analysis of static and dynamic behavior is a task of intense research. Many research activities have been devoted toward the development of theoretical and computational methods for the appropriate analysis of such members.

The first consistent study dealing with the static structural behavior of thin-walled composite-orthotropic members, under various loading patterns, was due to Bauld and Tzeng (1984), who developed, invoking Vlasov hypotheses, a beam theory to analyze fiber-reinforced members featuring open cross-sections with symmetric laminates. Although this theory assumed the cross-sections to be shear undeformable and it was restricted to structural members constructed with non-general stacking sequences and employed only for static analysis, further contributions from many authors until the present time, made it possible to extend Vlasov models by considering shear deformability due to bending, warping effects, etc. and the resulting models were employed in many problems, as it is described as follows.

Composite Thin-walled beam-models allowing for some effects of shear deformability were first presented, in the middle eighties (Giavotto et al. 1983 and Bauchau, 1985). In these works the effect of shear deformability and specially the warping torsion shear deformability was not taken into account or was slightly studied in a few problems of static's and dynamics.

The late eighties and the nineties brought a considerable amount of new models and uses. Some researchers (Rehfield et al. 1990; Librescu and Song, 1992; Song and Librescu, 1993; Na and Librescu, 2001) studied the non-conventional effects of constitutive elastic couplings (such as bending-bending coupling or bending-shear coupling, etc) in the mechanics of cantilever boxed-beams only considering the bending component of shear flexibility whereas the warping torsion component of shear flexibility was neglected. However in these models new extensions were performed, such as the accounting for the effect of thickness in shear and warping deformations, as well as new studies devoted to the dynamical aspects of elastic couplings, among others.

By making use of the Hellinger-Reissner principle, the authors of the present paper introduced recently (Cortínez and Piovan, 2002) a theory of thin-walled beams with symmetric balanced laminates, which considers full shear flexibility. The model covered topics of dynamics under states of initial normal stresses, and also accounted for thickness shear flexibility and warping.

Many of the aforementioned models were employed for eigenvalue calculation, among other uses. However, these models considered only beams with uniform cross-section. Although, there are some works devoted to the free vibration analysis of tapered beams with solid cross-section made of composite materials (Rao and Ganesan, 1995), however despite the importance in robotic arms and rotor-blades, there is no evidence of studies focused in the free vibrations of thin-walled tapered beams made of composite materials.

In the present work, a power series methodology is employed to calculate the free vibration frequencies of composite thin-walled tapered beams allowing shear flexibility due to bending as well as due to warping torsion. Several studies are performed in box-beams with special lamination. The effect of taper is analyzed and its influence in the free vibration appropriately enhanced.

2 BRIEF REVIEW OF THE MODEL

In Figure 1 a sketch of a thin-walled beam is shown. In this figure, it is possible to see the reference points ***C*** and ***B***. The principal reference point ***C*** is located at the geometric center of the cross-section, where the axis x is parallel to the longitudinal axis of the beam, while y and z are the axes associated to the cross section, but not necessarily the principal ones. The point ***B*** is a generic point belonging to the middle line of the cross-sectional wall (see Figure 2.a); its co-ordinates are denoted as *Y(s)* and *Z(s)*. The Figure 2.b shows the displacement parameters of the model.

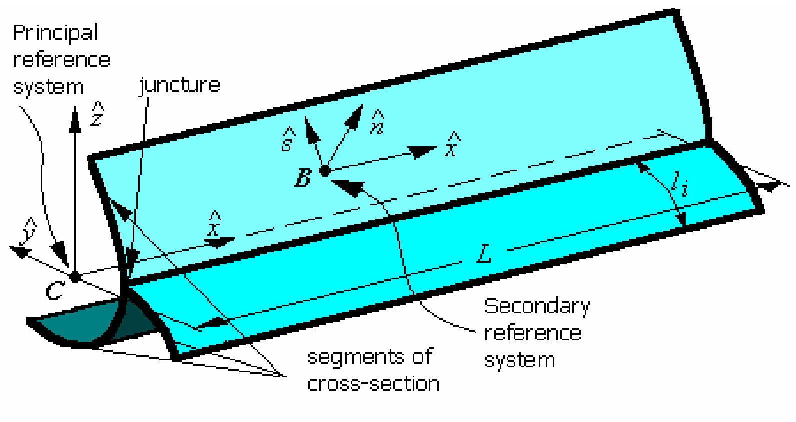

Figure 1: Sketch of a general straight thin-walled beam

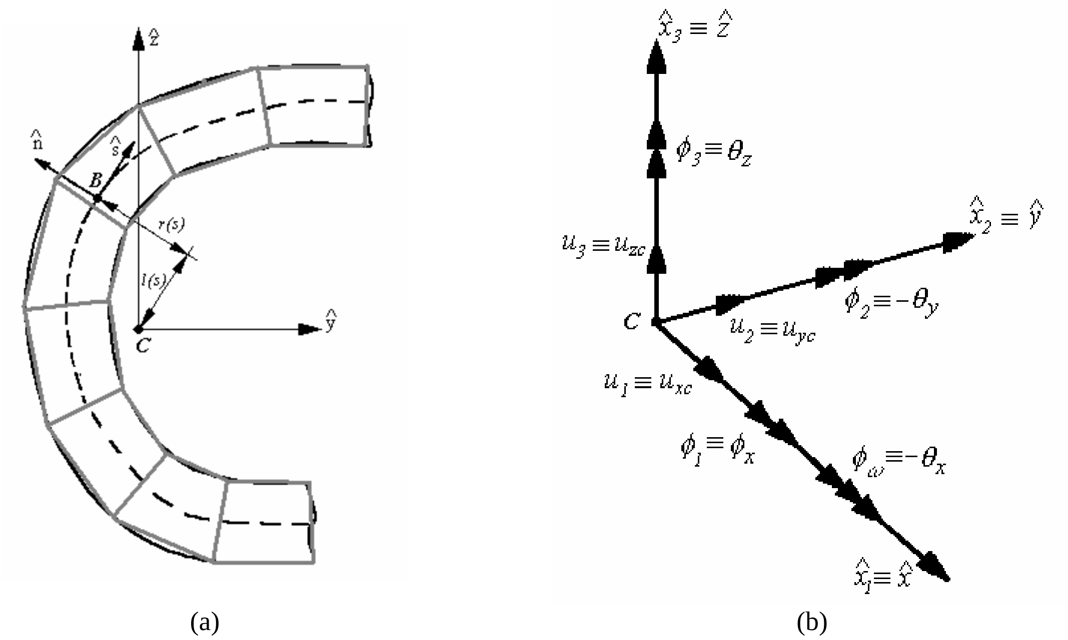

Figure 2: (a) Description of cross-section geometrical entities and (b) displacement parameters

The beam model employed in this study was developed (Piovan, 2003) under the following hypotheses: (a) the cross-section contour is rigid in its own plane; (b) the warping distribution is assumed to be given by the Saint-Venant function for isotropic beams; (c) shell force and moment resultant corresponding to the circumferential stress σ_{ss} and the force resultant corresponding to σ_{ns} are neglected; (d) The radius of curvature at any point of the shell is neglected; (e) Twisting curvature of the shell is expressed according to the classical plate theory, but bending curvature is expressed according to the first order shear deformation theory; (f) the stacking sequence is of circumferentially uniform stiffness (or CUS); (g) the shear flexibility due to in-thickness strains is neglected. Under this context, the mechanics of a thin-walled beam model allowing for shear flexibility due to bending and warping can be defined with following differential equations (Cortinez and Piovan, 2002; Piovan, 2003):

$$
\begin{aligned}
&-\frac{\partial Q_X}{\partial x} + \overline{M}_1(x) = 0 \\
&-\frac{\partial Q_Y}{\partial x} + \overline{M}_2(x) = 0 \\
&\frac{\partial M_Z}{\partial x} - Q_Y + \overline{M}_3(x) = 0 \\
&-\frac{\partial Q_Z}{\partial x} + \overline{M}_4(x) = 0 \\
&\frac{\partial M_Y}{\partial x} - Q_Z + \overline{M}_5(x) = 0 \\
&-\frac{\partial}{\partial x}\left[T_{SV} + T_W\right] + \overline{M}_6(x) = 0 \\
&\frac{\partial B}{\partial x} - T_W + \overline{M}_7(x) = 0
\end{aligned}
\tag{1}
$$

Where, Q_X is the axial force; Q_Y and Q_Z are shear forces; M_Y and M_Z are bending moments, B is the bimoment, T_{SV} is the twisting moment due to pure torsion and T_W is the flexural-torsional moment, due to warping torsion. $\overline{M}_j$, $j = 1,\ldots,7$ are the inertial forces.

These differential equations are subjected to the following boundary conditions:

a) Clamped-Clamped

$$u_{xc} = u_{yc} = u_{zc} = \theta_z = \theta_y = \phi_x = \theta_x = 0 \text{ at } x = 0 \text{ and } x = L \tag{2}$$

b) Clamped-Free

$$
\begin{aligned}
Q_X = Q_Y = Q_Z = M_Y = M_Z = T_{SV} + T_W = B = 0 \text{ at } x = 0 \\
u_{xc} = u_{yc} = u_{zc} = \theta_z = \theta_y = \phi_x = \theta_x = 0 \text{ at } x = L
\end{aligned}
\tag{3}
$$

In the previous equations, u_{xc} is the axial displacement of the centroid, u_{yc} and u_{zc} are lateral displacements of the centroid, θ_y and θ_z are the bending rotation parameters, ϕ_x is the twisting angle and θ_x is a warping intensity parameter.

For a circumferentially uniform stiffness lamination, the aforementioned beam-stress-resultants are related to the displacement variables by means of the following expression (Piovan, 2003):

$$\begin{Bmatrix} Q_X \\ M_Y \\ M_Z \\ B \\ Q_Y \\ Q_Z \\ T_W \\ T_{SV} \end{Bmatrix} = \begin{bmatrix} J_{11}^{11} & 0 & 0 & 0 & 0 & 0 & J_{17}^{16} & J_{18}^{16} \\ & J_{22}^{11} & 0 & 0 & J_{25}^{16} & 0 & 0 & 0 \\ & & J_{33}^{11} & 0 & 0 & J_{36}^{16} & 0 & 0 \\ & & & J_{44}^{11} & 0 & 0 & 0 & 0 \\ & & & & J_{55}^{66} & 0 & 0 & 0 \\ & & sym & & & J_{66}^{66} & 0 & 0 \\ & & & & & & J_{77}^{66} & J_{78}^{66} \\ & & & & & & & J_{88}^{66} \end{bmatrix} \begin{Bmatrix} u'_{xc} \\ -\theta'_y \\ -\theta'_z \\ -\theta'_x \\ u'_{yc} - \theta_z \\ u'_{zc} - \theta_y \\ \phi'_x - \theta_x \\ \phi'_x \end{Bmatrix} \quad (4)$$

and the inertia terms are expressed as follows

$$\begin{Bmatrix} \overline{M}_1 \\ \overline{M}_2 \\ \overline{M}_3 \\ \overline{M}_4 \\ \overline{M}_5 \\ \overline{M}_6 \\ \overline{M}_7 \end{Bmatrix} = \begin{bmatrix} J_{11}^{\rho} & 0 & 0 & 0 & 0 & 0 & 0 \\ & J_{11}^{\rho} & 0 & 0 & 0 & 0 & 0 \\ & & J_{33}^{\rho} & 0 & 0 & 0 & 0 \\ & & & J_{11}^{\rho} & 0 & 0 & 0 \\ & & & & J_{22}^{\rho} & 0 & 0 \\ & sym & & & & J_{22}^{\rho} + J_{33}^{\rho} & 0 \\ & & & & & & J_{44}^{\rho} \end{bmatrix} \begin{Bmatrix} \ddot{u}_{xc} \\ \ddot{u}_{yc} \\ \ddot{\theta}_z \\ \ddot{u}_{zc} \\ \ddot{\theta}_y \\ \ddot{\phi}_x \\ \ddot{\theta}_x \end{Bmatrix} \quad (5)$$

the stiffness coefficients in (3) and the inertia coefficients in (4) are obtained as follows:

$$\begin{gathered} J_{ij}^{kh} = \int_S \left[\overline{A}_{kh} \left(\overline{g}_i^{(a)} \overline{g}_j^{(a)} \right) + \overline{B}_{kh} \left(\overline{g}_i^{(a)} \overline{g}_j^{(c)} + \overline{g}_i^{(c)} \overline{g}_j^{(a)} \right) + \overline{D}_{kh} \left(\overline{g}_i^{(c)} \overline{g}_j^{(c)} \right) \right] ds \\ J_{ij}^{\rho} = \int_A \rho \, \overline{g}_i^{(d)} \overline{g}_j^{(d)} dsdn \end{gathered} \quad (6)$$

where the vectors $\overline{g}^{(j)}$ are defined as follows:

$$\begin{gathered} \overline{g}^{(a)} = \left\{ 1, Z(s), Y(s), \omega_P, \frac{dY}{ds}, \frac{dZ}{ds}, r(s) + \psi(s), \psi(s) \right\}, \overline{g}^{(b)} = \left\{ 0,0,0,0, \frac{dZ}{ds}, -\frac{dY}{ds}, -l(s), 0 \right\} \\ \overline{g}^{(c)} = \left\{ 0, \frac{dY}{ds}, -\frac{dZ}{ds}, l(s), 0, 0, 1, -2 \right\}, \ \overline{g}^{(d)} = \left\{ 1, Z(s) + n\frac{dY}{ds}, Y(s) - n\frac{dZ}{ds}, \omega(s) \right\} \end{gathered} \quad (7)$$

In the equation (6), ρ is the density and $\overline{A}_{ij}$, $\overline{B}_{ij}$ and $\overline{D}_{ij}$ are elastics coefficients (Piovan, 2003), whereas ω is the whole warping function, which is composed by two terms: primary or contour warping (ω_p) and secondary or thickness warping (ω_s) defined by:

$$\begin{gathered} \omega = \omega_p(s) + \omega_s(s,n) \\ \omega_p(s) = \int_{s_0}^{s} \left[r(s) + \psi(s) \right] ds + D_C, \quad \omega_s(s,n) = n\, l(s) \end{gathered} \quad (8)$$

The function $\psi(s)$ is the torsional shear flow with reference to a closed contour section. It accounts for variable laminates along the contour and it is defined as follows:

$$\psi(s) = \frac{1}{\overline{A}_{66}(s)}\left[\frac{\int_s r(s)\,ds}{\oint_S \frac{1}{\overline{A}_{66}(s)}\,ds}\right], \quad D_C = \frac{\oint_S [r(s)+\psi(s)]\overline{A}_{11}(s)ds}{\oint_S \overline{A}_{11}(s)ds} \tag{9}$$

$r(s)$ and $l(s)$ are defined as follows:

$$r(s) = -Z(s)\,\frac{dY}{ds} + Y(s)\,\frac{dZ}{ds}, \quad l(s) = Y(s)\,\frac{dY}{ds} + Z(s)\,\frac{dZ}{ds} \tag{10}$$

It is interesting to note that the CUS lamination provides a selective elastic coupling. As it can be seen in (3) and (4), the axial equation is coupled with the torsion and warping equations, on the other hand the four equations of bending are coupled among them.

3 POWER SERIES METHODOLOGY

In order to develop the solution, one has to describe each displacement function by means of power series, this requires a previous non-dimensional re-definition of the domain (i.e. $0 \le \overline{x} \le 1$, with $\overline{x} = x/L$, Filipich et al, 2003a,b):

$$\begin{gathered} u_{xc} = \sum_{i=0}^{M} a_{1i}\overline{x}^i \\ u_{yc} = \sum_{i=0}^{M} a_{2i}\overline{x}^i\ , \theta_z = \sum_{i=0}^{M} a_{3i}\overline{x}^i \\ u_{zc} = \sum_{i=0}^{M} a_{4i}\overline{x}^i\ , \theta_y = \sum_{i=0}^{M} a_{5i}\overline{x}^i \\ \phi_x = \sum_{i=0}^{M} a_{6i}\overline{x}^i\ , \theta_x = \sum_{i=0}^{M} a_{7i}\overline{x}^i \end{gathered} \tag{11}$$

Theoretically, $M \to \infty$, however for practical purposes M is a large arbitrary integer. Now, the successive derivatives of the displacement functions, u_{xc} for instance, can be expressed as:

$$u_{xc}^{(n)} = \sum_{i=0}^{M-n} \varphi_{ni} a_{1,i+n}\overline{x}^i, \quad n = 1,2,3,... \text{ with } \varphi_{ni} \equiv \frac{(i+n)!}{i!} = (i+1)(i+2)...(i+n) \tag{12}$$

Now the unknowns of the problem are a_{ji}, $j = 1,...,7$, $i = 0,...,M$, that is an amount of $7(M+1)$ unknowns.

It has to keep in mind that in this problem the cross-section properties vary continuously with $\overline{x}$ leading to a differential system with variable coefficients, consequently one has to employ series products. Thus, if $h_1(\overline{x}), h_2(\overline{x}), h_3(\overline{x})$ are analytical functions defined as:

$$h_k = \sum_{i=0}^{M} c_{k,i}\overline{x}^i, \quad k = 1,2,3 \tag{13}$$

and if $h_1(\bar{x}), h_2(\bar{x}), h_3(\bar{x})$ are such that the product $h_3 = h_1 h_2$, then

$$c_{3,i} = \sum_{r=0}^{i} c_{1,r} c_{2,i-r} \bar{x}^i = \sum_{r=0}^{i} c_{2,r} c_{1,i-r} \bar{x}^i \tag{14}$$

Finally, an integer power of the independent variable $\bar{x}$ can be described by means a power series as:

$$x^m = \sum_{i=0}^{M} b_{m,i} \bar{x}^i, \quad m = 1,2,3,\dots \text{ with } b_{m,i} = \delta_{m,i} = \delta_{i,m} \tag{15}$$

where, $\delta_{i,m}$ and $\delta_{m,i}$ are second order Kronecker deltas.

Substituting (11) in the differential system (1), taking into account (12)-(15), considering the boundary conditions (2) and performing a suitable algebraic manipulation, it is possible to obtain the algebraic homogeneous linear system, in the following canonical form:

$$\boldsymbol{A} - \lambda^2 \boldsymbol{B} = \boldsymbol{0}, \text{ with } \lambda^2 = \rho\, \Omega^2 e L \tag{16}$$

where Ω is the natural circular frequency.

4 NUMERICAL STUDIES AND ANALYSIS

Figure 3.a shows a tapered box beam where the height varies according to expression (17), and with h_0 as the largest height. Figure 3.b shows the CUS lamination in the cross-section. In Table 1 one can see the properties of the graphite fiber reinforced epoxy AS4/3501-6 composite material. The geometrical dimensions of the specimen are: length, $L = 1.00\ m$; height, $h_0 = 0.100\ m$; width, $b = 0.050\ m$ and thickness, $e = 0.003\ m$.

$$h(\bar{x}) = h_0 + \alpha_H \bar{x} \tag{17}$$

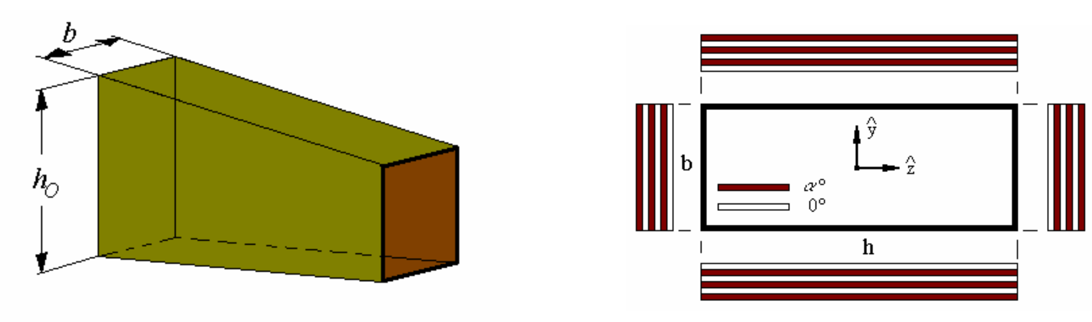

(a) (b)

Figure 3: (a) Box Beam under study (b) CUS lamination

E_1 = 144 GPa, E_2 = 9.68 GPa
$G_{12} = G_{13}$ = 4.14 GPa G_{23} = 3.45 GPa
ν_{12} = 0.3 ν_{23} = 0.5
ρ = 1389 Kg/m^3

Table 1: Properties of AS4/3506-1.

In the case of uniform cross-sectional properties along the length, it is possible to perform a comparison of the present approach with other methods. Thus Table 2 shows the first five circular frequencies of a clamped-clamped beam for different angles of fiber orientation (α), comparing the results obtained with power series and a finite element methodology (Piovan, 2003). As it can be seen the comparison is quite good and the discrepancies are no longer than 0.1%. The eigenvalues were obtained with series of $M=100$ terms and with models of 60 finite elements.

α	Method	Ω_1	Ω_2	Ω_3	Ω_4	Ω_5
0	Series	2665	3934	4309	5455	7949
	FEM	2665	3934	4304	5468	7956
15	Series	3047	4600	5375	6836	9261
	FEM	3048	4611	5368	6841	9278
30	Series	3135	4941	6814	7408	10562
	FEM	3136	4943	6806	7413	10574
45	Series	2939	4622	6506	6776	10129
	FEM	2940	4623	6512	6780	10135
60	Series	2687	4157	5380	5962	8919
	FEM	2688	4158	5383	5965	8925
75	Series	2470	3765	4555	5325	7885
	FEM	2470	3765	4557	5328	7890
90	Series	2381	3614	4272	5084	7491
	FEM	2383	3611	4273	5086	7500

Table 2: Natural Frequencies of a uniform clamped-clamped beam.

Tables 3 and 4 show the variation of the first five natural frequencies of a clamped-clamped beam with respect to the fiber orientation angle, for slopes of $\alpha_H=-0.025$ and $\alpha_H=-0.050$, respectively. Figures 4 and 5 depict the variation of the first and second frequencies of the clamped-clamped beam with respect to the fiber orientation angle, for three different slopes. The mode associated to the first frequency is flexural dominant in the y-direction, whereas the mode associated to the second frequency is flexural dominant in the z-direction. The bending modes in *y*- and *z*-directions are decoupled if the reinforcing fibers are oriented along or perpendicular to the beam axis. However, if the fibers are oriented in any other angle than $0°$ or $90°$ the flexural modes are coupled between them, as it can be seen from equation (4). Figure 6 shows the variation of the third frequency of the clamped-clamped beam with respect to the fiber orientation angle, for three different slopes. The mode associated to the third frequency is torsional dominant coupled with the axial motion, when the fiber orientation angle is other than $0°$ or $90°$. For a uniform beam and the fiber orientation angle $\alpha = 30°$, Figures 7, 8 and 9 offer examples of the modes associated to the first, second and third frequencies, respectively.

Observing Figures 4, 5 and 6, it is interesting to note that the behavior of the first and third frequencies manifests a growth with the increase of the tapering, for all fiber orientation.

Conversely, the values of the second frequency are lower with increasing values of the taper ratio.

α	Ω_1	Ω_2	Ω_3	Ω_4	Ω_5
0	2735	3755	4427	5645	7643
15	3091	4352	5693	6951	9042
30	3142	4575	7482	10146	12946
45	2950	4274	6885	9601	11604
60	2717	3876	5585	6093	8454
75	2510	3538	4722	5463	7513
90	2426	3404	4406	5224	7165

Table 3: Natural Frequencies of clamped-clamped beam, for slope of α_H =*-0.025*.

α	Ω_1	Ω_2	Ω_3	Ω_4	Ω_5
0	2803	3509	4527	5841	7220
15	3118	4007	5764	7022	8658
30	3147	4118	7513	9476	12885
45	2958	3837	6968	8833	11829
60	2734	3514	5760	6214	7827
75	2540	3239	4798	5601	7008
90	2461	3128	4512	5365	6697

Table 4: Natural Frequencies of clamped-clamped beam, for slope of α_H =*-0.050*.

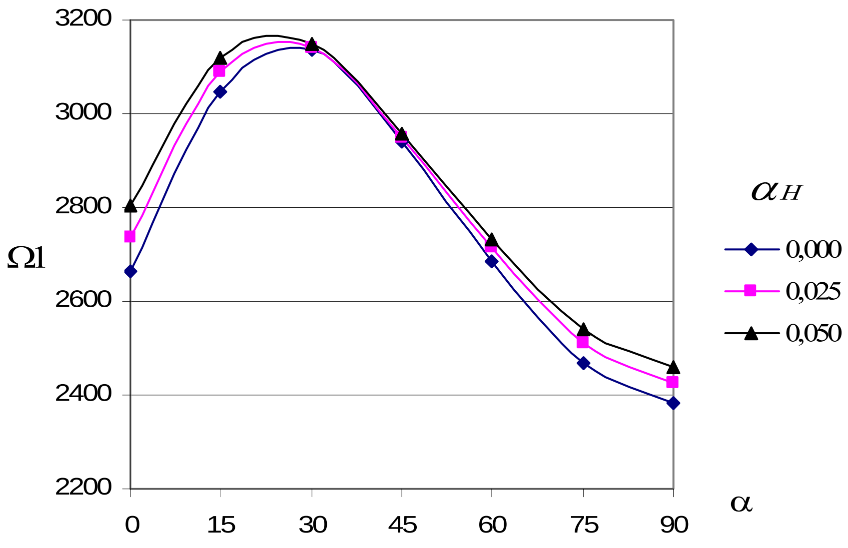

Figure 4: Variation of first frequency with the orientation angle, for a clamped-clamped beam

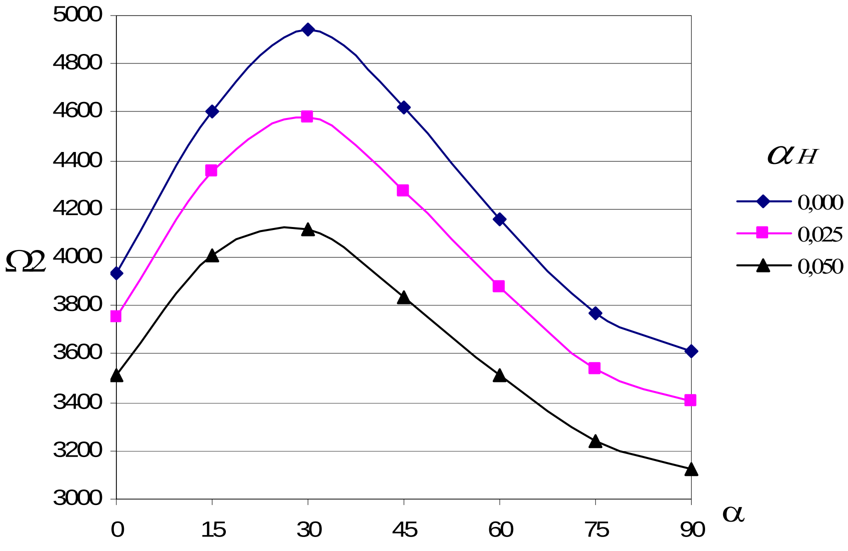

Figure 5: Variation of second frequency with the orientation angle, for a clamped-clamped beam

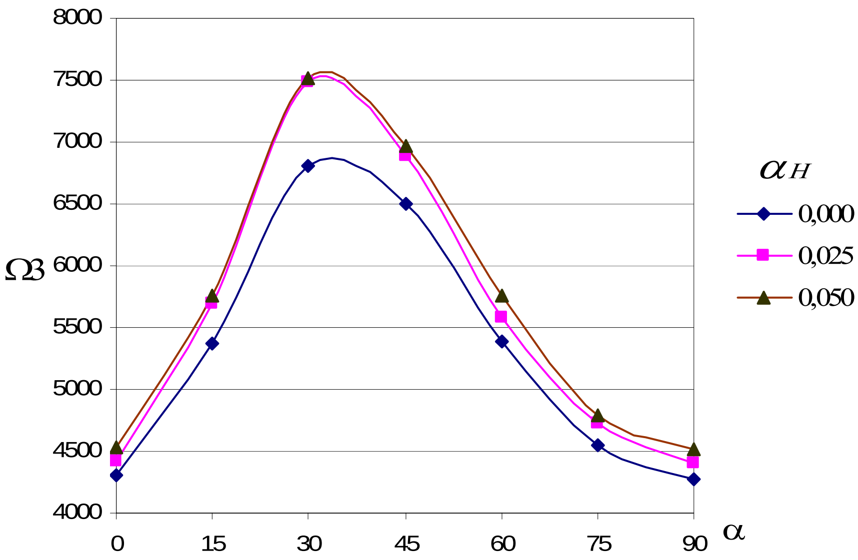

Figure 6: Variation of the third frequency with the orientation angle, for a clamped-clamped beam

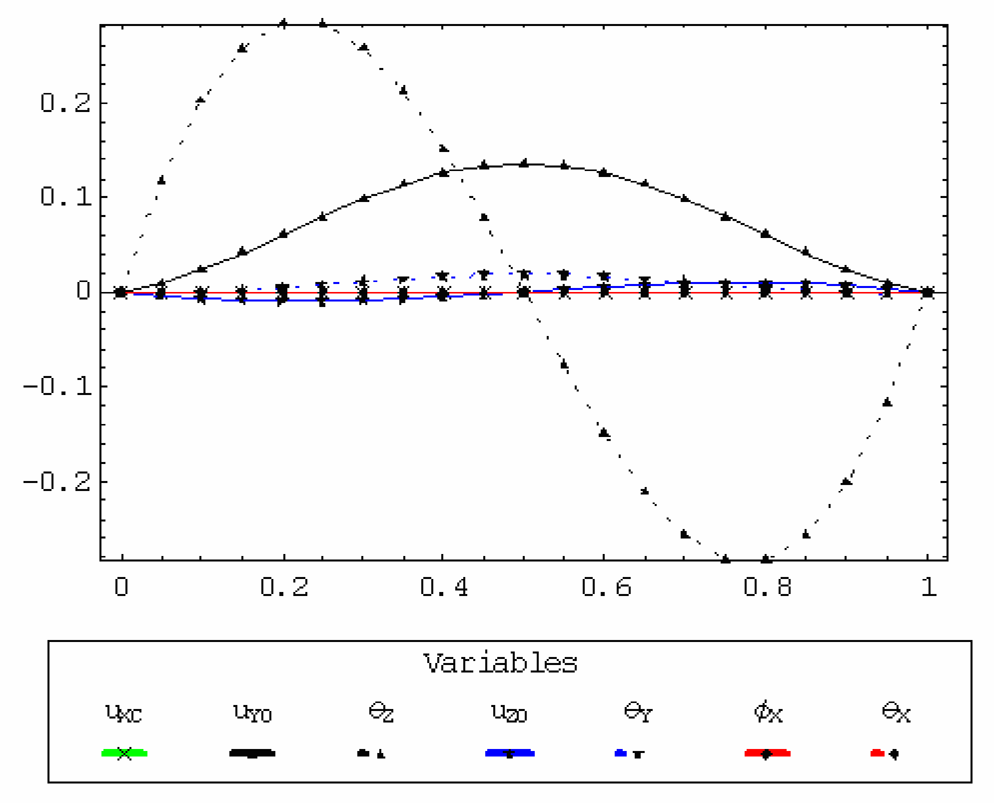

Figure 7: Bending mode associated to the first frequency, for a clamped-clamped uniform beam

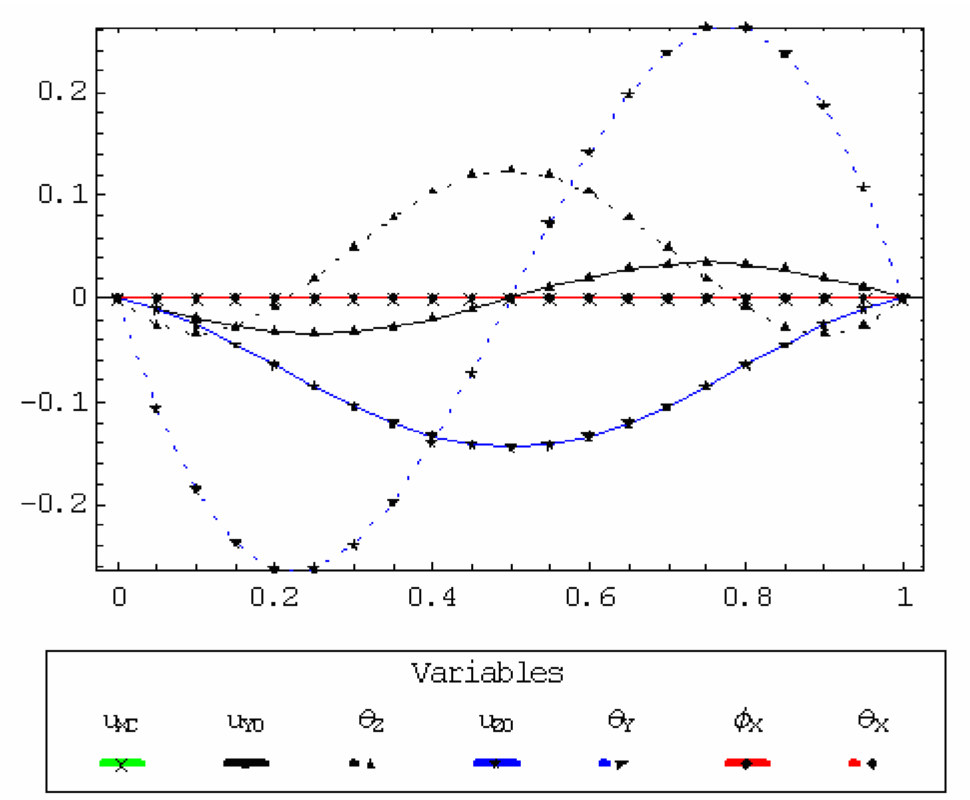

Figure 8: Bending mode associated to the second frequency, for a clamped-clamped uniform beam

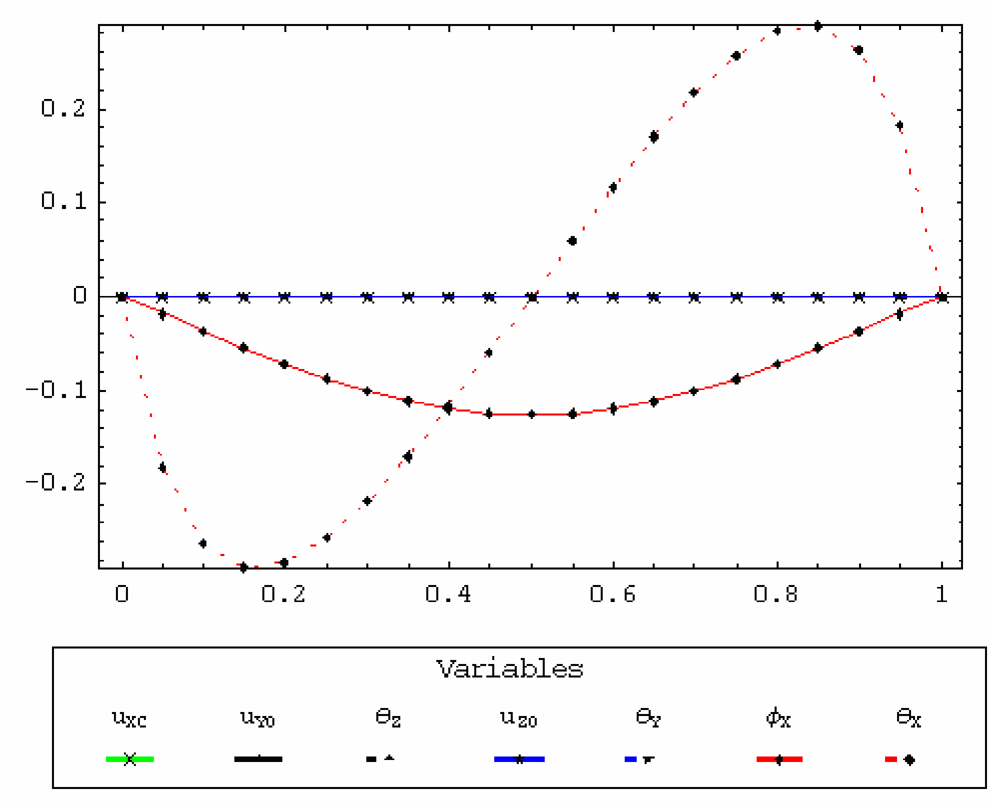

Figure 9: Torsional mode associated to the third frequency, for a clamped-clamped uniform beam

5 CONCLUSIONS

In this article the free vibrations of thin-walled tapered box-beams constructed with composite materials were analyzed. Laminates providing special elastic couplings, like Circumferentially Uniform Stiffness stacking sequences were employed. The effect of tapering in the free vibrations of composite thin walled box-beam was analyzed. The calculation is performed by means of a power series methodology which can give eigenvalues of arbitrary precision. In the calculation of eigenvalues of composite beams with tapered geometries or other functional variation along the domain, this methodology can offer advantages with respect to common finite element methodologies where the elements have constants properties along the their length, and a very fine mesh has to be used to get accurate results.

6 ACKNOWLEDMENTS

The authors sincerely recognize the support of Secretaria de Ciencia y Tecnología de la Universidad Tecnológica Nacional and CONICET.

REFERENCES

E.J. Barbero. *Introduction to Composite Material Design*. Taylor and Francis Inc. 1999.
O.A. Bauchau. A Beam Theory for Anisotropic Materials. *Journal of Applied Mechanics* 52(2):416-422, 1985.
N.R. Bauld Jr. and L.S. Tzeng. A Vlasov theory for fiber-reinforced beams with thin-walled open cross sections. *International Journal of Solids and Structures*, 20(3):277-297, 1984.
V.H. Cortínez and M.T. Piovan, Vibration and buckling of composite thin-walled beams with

shear deformability. *Journal of Sound and Vibration*, 258(4):701-723, 2002.

R.M. Jones. *Mechanics of Composite Materials*. Taylor and Francis Inc. 1999.

R.K. Kapania and S. Raciti. Recent Advances in Analysis of Laminated Beams and Plates: 1-Shear Effects and Buckling. *AIAA Journal* 27(7):923-934, 1989.

V. Giavotto M. Borri, L. Mantegaza and G. Ghiringhelli, V. Carmaschi, G.C. Maffioli and F. Mussi. Anisotropic Beam Theory and Applications. *Computers and Structures* 16:403-413, 1983.

L.W. Rehfield, A.R. Atilgan and D.H. Hodges. Non-classical behavior of Thin-Walled Composite Beams with closed cross-sections. *Journal of American Helicopter Society* 35(3):42-50, 1990.

L. Librescu and O. Song. On the aeroelastic tailoring of composite aircraft swept wings modeled as thin walled beam structures. *Composites Engineering*, 2(5-7):497-512, 1992.

O. Song and L. Librescu. Free vibration of anisotropic composite thin-walled beams of closed cross-section contour. *Journal of Sound and Vibration*, 167(1):129-147, 1993.

S Na and L Librescu. Dynamic response of elastically tailored adaptive cantilevers of non-uniform cross section exposed to blast pressure pulses. *International Journal of Impact Engineering* 25(9):847-867, 2001.

C.P. Filipich, M.R. Escalante and M.B. Rosales, Series de potencias: una ventajosa alternativa aplicada a vibraciones libres de pórticos, *Mecánica Computacional* 22:908-920, 2003a.

C.P. Filipich, M.B. Rosales and F.S. Buezas, Vibración libre de arcos simétricos de directriz arbitraria resueltos por medio de series de potencias, *Mecánica Computacional* 22:892-907, 2003b.

M.T. Piovan. *Estudio Teórico y Computacional sobre la Mecánica de Vigas Curvas de Materiales Compuestos, con Paredes delgadas, considerando efectos no convencionales*, PhD Dissertation, Universidad Nacional del Sur, Bahía Blanca, Argentina, 2003.

S.R. Rao and N. Ganesan. Dynamic-Response of Tapered Composite Beams Using Higher-Order Shear Deformation-Theory. *Journal of Sound and Vibration* 187(5):737-756, 1995.